OVERVIEW OF CMS RESULTS — RECENT HIGHLIGHTS*

Barbara Clerbaux

on behalf of the CMS Collaboration

IIHE-ULB, Université Libre de Bruxelles, ULB, Brussels, Belgium
barbara.clerbaux@cern.ch

(Received July 9, 2021; accepted July 12, 2021)

In these proceedings, highlights of the CMS experiment are presented, with a focus on the latest results obtained when analysing the whole LHC Run 2 dataset. The presentation of the CMS results is divided into three main parts. The first one is dedicated to Standard Model measurements as a probe for new physics, with, in particular, the presentation of multi-boson production results. The second part covers the latest Higgs boson measurements in various decay channels, with a focus on the recent CMS observation of the Higgs boson decay to a pair of muons. The last part presents a selection of few results on direct searches for new physics.

DOI:10.5506/APhysPolB.52.889

1. Introduction

At the date of 2020-12-17, a total of 1015 collider data papers has been published (or submitted) by the CMS Collaboration, passing the impressive symbolic number of one thousand. In addition to standard high-energy physics journal publications, several CMS papers have now been accepted in dedicated machine learning journals, showing the development of such a tool inside the collaboration. The majority of the CMS Collaboration recent publications is now based on the entire Run 2 data set (data taken in years 2016–2018), corresponding to a total integrated luminosity of 137 fb^{-1}. In these proceedings, a selection of the latest CMS results (mainly published in 2020 or 2021) is presented. The proceedings are organised as follows. The first section is devoted to the presentation of the LHC Run 1 and Run 2, followed by a description of the CMS Run 2 data taking and the so-called legacy samples. Finally, the recent CMS tool developments are given, moving from multi-variable analysis (MVA) to deep neural network (DeepNN).

---

* Presented at XXVII Cracow Epiphany Conference on *Future of Particle Physics*, Cracow, Poland, January 7–10, 2021.

The second section concerns results on Standard Model (SM) measurements. It includes various new multi-boson production results: the production of polarised same-sign WW pairs, electroweak $W\gamma$ production, the first observation of VVV production. The first measurement of top pair and charm quark is also detailed. The third section is dedicated to the H sector. After the presentation of the latest results on the H boson mass measurement, recent results on the H couplings to fermions are given in more detail, with a focus on the impressive observation of the $H \to \mu\mu$ decay. Update on $H \to \gamma\gamma$, $H \to \tau\tau$, and boosted $H \to bb$ decay modes is also reported. A selection of results of direct searches for new physics is the subject of the fourth section. Two recent SUSY results are described: the electroweak and strong production with dilepton final states and stop-quark pair production in dilepton final states, followed by the search for long-lived particles decaying into displaced jets and, finally, the search for dark photons in vector boson fusion (VBF) production. The last section of the proceedings gives a short description of the CMS activities during the second Long Shutdown period (LS2) in 2019–2021, as well as plans for the Run 3 data taking, expected to start in 2022.

1.1. The LHC Run1 and Run 2

The Large Hadron Collider (LHC) at CERN provides proton–proton (pp) interactions at high energy (in special runs, the proton beam(s) may be replaced by ion (lead) beam(s)). After the Run 1 data taking period (years 2010–2012, at the pp centre-of-mass energy of 7 and 8 TeV), the LHC machine was upgraded in order to provide collisions at higher energy (13 TeV). The Run 2 took place in the years 2015–2018. The LHC delivered an important amount of data in years 2016–2018 as it can be seen in Fig. 1. The LHC luminosity increase implies an augmentation of the pile-up (PU) effect, a superposition of several pp interactions in the same beam bunch crossing. During the Run 2 period, the average mean number of interactions per bunch crossing was 34.

1.2. CMS Run 2 data taking and legacy samples

Four experiments are placed at the LHC collider: the two multi-purpose experiments ATLAS and CMS, as well as LHCb (focussed on B hadron measurements) and ALICE (dedicated to heavy-ions physics). A detailed description of the CMS detector is presented in Ref. [1]. During the Run 2 data taking period, CMS operated using various triggers: *(i)* the standard triggers using leptons, jets vertexing or missing transverse energy (MET), *(ii)* B-parking triggers in the year 2018 which store data with lower trigger threshold and which are delayed in their processing, in order to accumulate 11B events enriched in unbiased B meson decays, *(iii)* scouting triggers which have lower transverse momentum (p_{T}) threshold and mass selections thanks to a reduction of event size to O(10 kB) with physics objects reconstructed only at the high level triggers (HLT), *(iv)* triggers for special dedicated runs as heavy-ion triggers and low-PU triggers. In these proceedings, events selected using the standard triggers are presented, as they are the ones used in the latest CMS publications. The CMS physicists dedicated important efforts toward the production of "legacy samples" for the full Run 2 dataset, with consistent reprocessing and final calibrations, with alignment and improvement in the simulation of detector conditions. As an example, improvement of the legacy electron reconstruction compared to the so-called "end-of-year" calibration can be seen in Fig. 2, presenting the di-electron mass resolution as a function of the pseudo-rapidity η, together with the impressive data/simulation agreement for the electron azimuthal angle distribution using Drell–Yan events at the Z boson peak; see Refs. [2–4] for more details.

1.3. CMS performance: from MVA to DeepNN

Machine learning algorithms in particular deep neural networks (DeepNN) are more and more used in CMS when relevant, due to their suitability to complex multi-classification problems. In this section, two recent CMS developments are presented. The first one concerns a new tau lepton identification tagger called "DeepTau". It is a multiclass tau lepton identification algorithm based on a convolutional deep neural network. It combines information from the high-level reconstructed tau lepton features together with the low-level information from the inner tracker, calorimeters and muon sub-detectors [5]. The second one, called DeepJet, is optimised

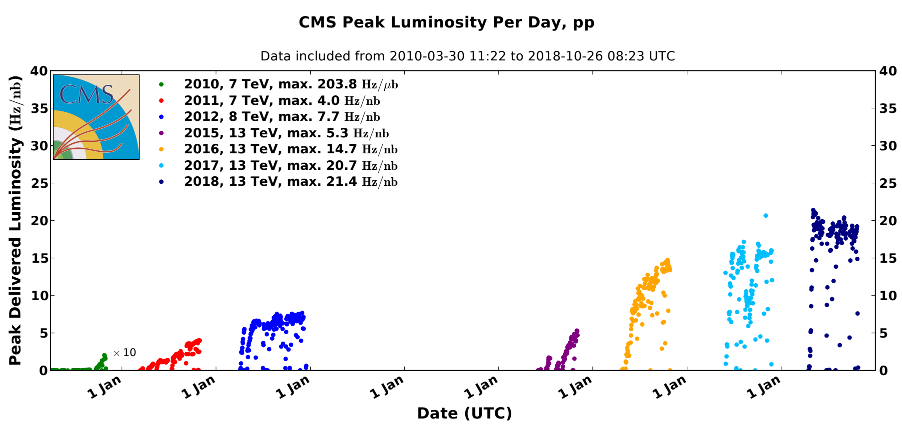

Fig. 1. Peak delivered luminosity per day as a function of time for the Run 1 (2010–2012) and the Run 2 (2015–2018) periods.

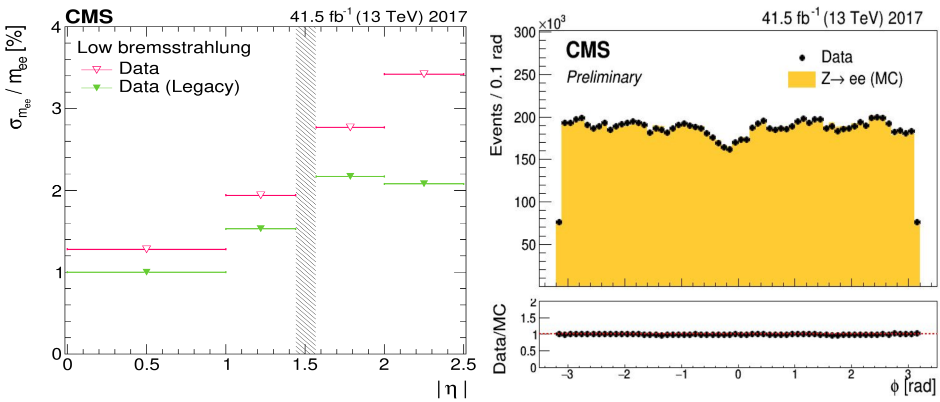

Fig. 2. Left: dielectron mass resolution (from Drell–Yan events at the Z boson peak) for legacy calibration compared to the end-of-year reconstruction [3]; Right: data *versus* simulation comparison for the electron azimuthal angle distribution [4].

for the identification of jets originating from b quarks. A deep neural network algorithm is based on 16(8) properties of up to 25 charged(neutral) particle-flow jet constituents, as well as 12 properties of up to 4 secondary vertices associated with the jet [6]. The performance of the DeepTau and DeepJet algorithm using 41.9 fb^{-1} of pp data collected in 2017 is presented in Fig. 3.

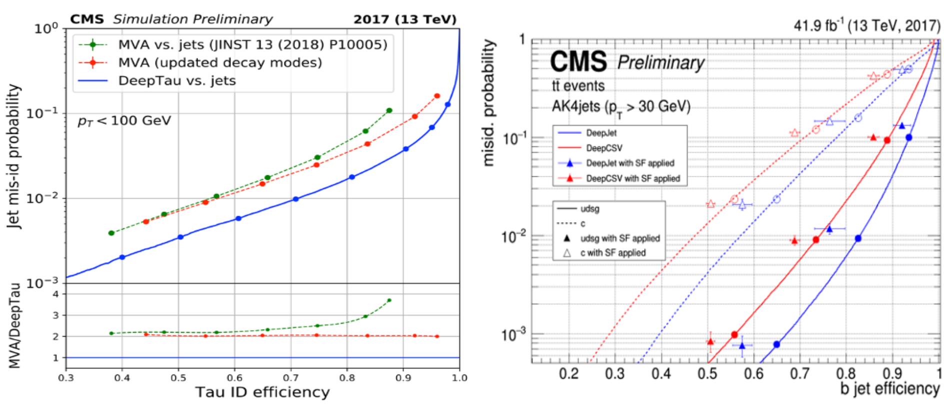

Fig. 3. Left: performance of the new tau-tagger algorithm (DeepTau) compared to the previous tagger based on the multi-variate analysis (MVA) tool. The plot shows the probability of mis-identification of a light jet as a tau jet as a function of the tau-tagging efficiency [5]; Right: performance of the new b-tagging algorithm (DeepJet) compared to the previous one (DeepCVS). The plot shows the probability of mis-identification of a light jet as a b jet as a function of the b-tagging efficiency [6].

2. SM measurements as probe for new physics

The CMS and ATLAS experiments have tested the SM through rare processes and differential cross-section measurements. Precise measurements of the SM production cross sections are important to prove a good control of the detector response and to estimate the various background contaminations from SM processes present in the searches for new physics. Figure 4 summarises the SM production cross sections measured by CMS for various processes: Z/W + jets production, diboson and triboson measurements, top sector and Higgs sector. Several of these measurements will be presented in the following. This impressive achievement has been possible due to the large dataset provided by the LHC and to the excellent reconstruction and calibration performance results, mentioned in the previous section.

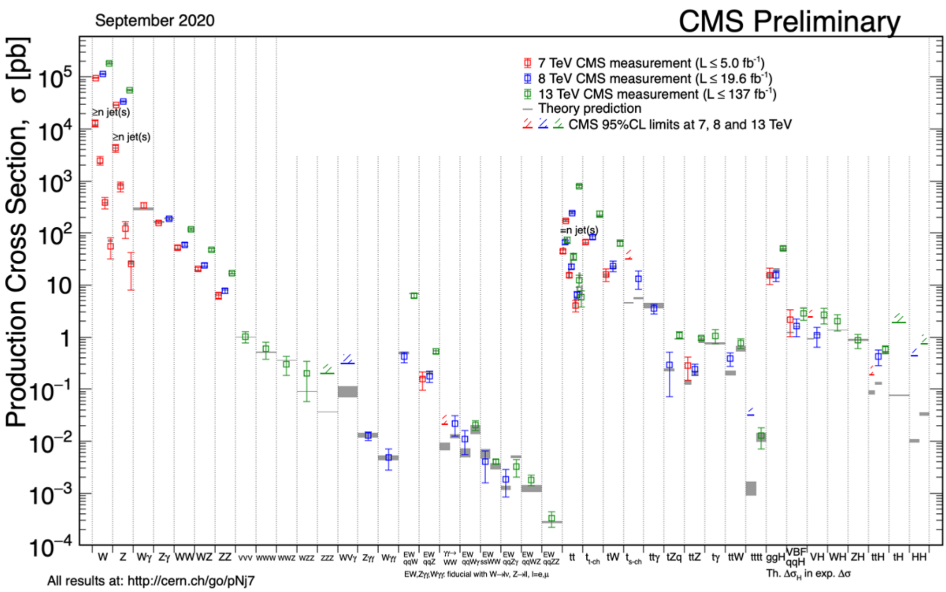

Fig. 4. Measurement of various Standard Model production cross sections at 7, 8 and 13 TeV.

2.1. *Production of polarised same-sign W-boson pairs*

The study of polarised WW pair production is an important measurement to test the electroweak symmetry breaking mechanism and to search for cross section modification as a hint for Beyond the SM (BSM) models, *i.e.* additional H scalar bosons. In the analysis, the production cross section of polarised same-sign W-boson pairs in association with two jets is measured, see Ref. [7]. Events are selected by requiring exactly two same-sign leptons (electrons or muons), moderate missing transverse momentum, and two jets with a large rapidity separation and a high dijet mass. Boosted decision trees (BDT) are used to separate between the polarised scattering processes by exploiting the kinematic differences. Several control regions are defined to constrain SM background contributions (WZ, tZq, ZZ). Two measurements are performed: first a simultaneous measurement of the $W^{\pm}_{\mathrm{L}}W^{\pm}_{\mathrm{L}}$ and $W^{\pm}_{\mathrm{X}}W^{\pm}_{\mathrm{T}}$ combination and then of the $W^{\pm}_{\mathrm{L}}W^{\pm}_{\mathrm{X}}$ and $W^{\pm}_{\mathrm{T}}W^{\pm}_{\mathrm{T}}$ combination, where the subscripts L and T stand for longitudinally and transversely polarised, X being L or T. The outputs of the BDT are presented in Fig. 5 for the two cases.

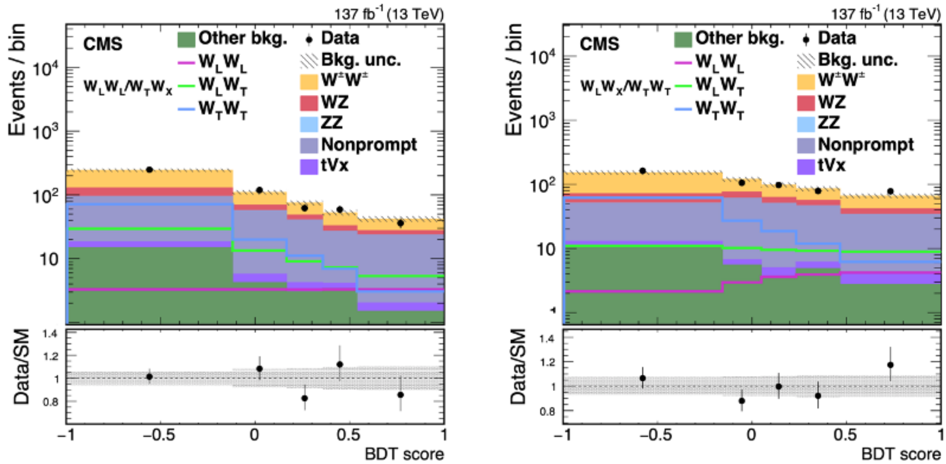

Fig. 5. Distributions of the output score of the signal BDT used for the $W^{\pm}_{\mathrm{L}}W^{\pm}_{\mathrm{L}}$ and $W^{\pm}_{\mathrm{X}}W^{\pm}_{\mathrm{T}}$ cross section measurement (left) and for the $W^{\pm}_{\mathrm{L}}W^{\pm}_{\mathrm{X}}$ and $W^{\pm}_{\mathrm{T}}W^{\pm}_{\mathrm{T}}$ cross section measurement (right) [7].

Results of the cross section measurements are given in Fig. 6. These are the very first measurements of polarised same-sign W-boson pair cross section. The electroweak production of at least one W_{L} is measured with 2.3 (3.1 exp.) standard deviations (σ). An upper limit at 95% C.L. of 1.17 (0.88 exp.) fb is set on the $W^{\pm}_{\mathrm{L}}W^{\pm}_{\mathrm{L}}$ production cross section.

Process	$\sigma\,\mathcal{B}$ (fb)	Theoretical prediction (fb)
$W^{\pm}_{\mathrm{L}}W^{\pm}_{\mathrm{L}}$	$0.32^{+0.42}_{-0.40}$	0.44 ± 0.05
$W^{\pm}_{\mathrm{X}}W^{\pm}_{\mathrm{T}}$	$3.06^{+0.51}_{-0.48}$	3.13 ± 0.35
$W^{\pm}_{\mathrm{L}}W^{\pm}_{\mathrm{X}}$	$1.20^{+0.56}_{-0.53}$	1.63 ± 0.18
$W^{\pm}_{\mathrm{T}}W^{\pm}_{\mathrm{T}}$	$2.11^{+0.49}_{-0.47}$	1.94 ± 0.21

Fig. 6. Measured fiducial cross sections for the $W_{\mathrm{L}}W_{\mathrm{L}}$ and $W_{\mathrm{X}}W_{\mathrm{T}}$ processes and for the $W_{\mathrm{L}}W_{\mathrm{X}}$ and $W_{\mathrm{T}}W_{\mathrm{T}}$ processes, for the helicity eigenstates defined in the parton–parton center-of-mass frame. The combination of the statistical and systematic uncertainties is shown [7].

2.2. Electroweak $W\gamma$ or ZZ production in association with 2 jets

Recently, CMS provided a first observation for the electroweak production of a W boson, a photon, and two jets [8]. The electron or muon W-boson decay modes are selected. The two jets are required to have a high dijet mass and a large separation in pseudorapidity. The observed (exp.) significance for this process is 4.9 (4.6)σ. After combining with previously reported CMS results at 8 TeV, the observed (exp.) significance is 5.3 (4.8)σ. The total cross section for $W\gamma$ production in association with 2 jets is in good agreement with recent theoretical predictions. In addition, constraints have been placed on anomalous quartic gauge couplings in terms of dimension-8 effective field theory operators.

Another search was performed for the electroweak production of two jets in association with two Z bosons this time, in the four-lepton final state, where electrons or muons are considered. The analysis is detailed in Ref. [9]. The electroweak cross section of ZZ + 2 jets is measured with an observed (exp.) significance of 4.0 (3.5)σ, and is in agreement with the SM prediction. Limits on anomalous quartic gauge couplings have been derived in terms of the effective field theory operators T0, T1, T2, T8, and T9.

2.3. Observation of VVV production

This subsection presents the first observation of the combined production of three massive gauge bosons (VVV with $V = W, Z$). This production mechanism allows to have access to triple gauge boson and quadruple gauge boson interaction, VVH and VVV interaction, and is sensitive to new particles coupling to V or modifying the SM couplings. The searches for individual WWW, WWZ, WZZ, and ZZZ production are performed in final states with 3 to 6 leptons (electrons or muons), or with two same-sign leptons, see Ref. [10]. Control regions are defined to estimate background contributions from data-driven methods. A cut-based and a BDT-based analyses are performed. Figure 7 presents a data *versus* SM expectation comparison for the various categories. The observed (exp.) significance of the combined VVV production signal is 5.7 (5.9)σ and the corresponding measured cross section relative to the SM prediction (the signal strength parameter μ) is $1.02\pm^{0.26}_{0.23}$. The significances of the individual WWW and WWZ production are 3.3 and 3.4σ, respectively. The signal strength results for the individual channels and for their combination are given in Fig. 8.

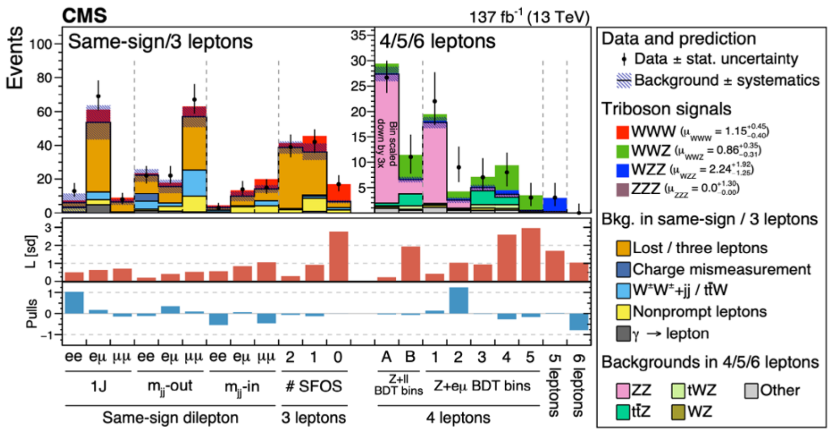

Fig. 7. Comparison of the observed numbers of events to the predicted yields. For the WWW and WWZ channels, the results from the BDT-based selections are used. The VVV signal is shown stacked on top of the total background [10].

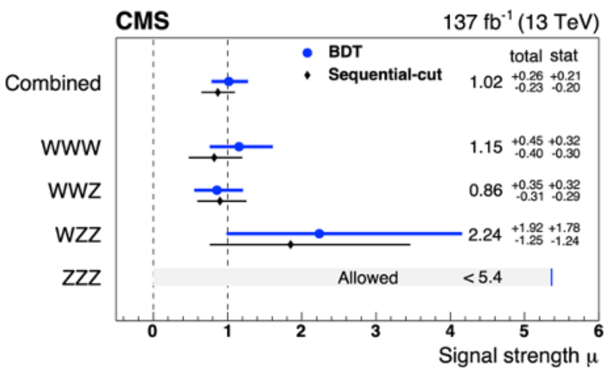

Fig. 8. (Colour on-line) Signal strengths for the BDT-based (grey/blue circles) and the cut-based (black circles) analyses. The error bars represent the total uncertainty. For ZZZ production, a 95% confidence level upper limit is shown [10].

2.4. Top-quark pair production with additional charm jets

The CMS Collaboration released a first measurement of the inclusive cross section for top-quark pairs produced in association with two additional charm jets, selecting dileptonic final states of the top-quark pair events, see Ref. [11]. A key aspect of the analysis is the development of a new charm jet identification algorithm (c tagging). This algorithm provides input to a neural network that is trained to distinguish among top-quark pair events with two additional charm ($ttcc$), bottom ($ttbb$), and light-flavour or gluon ($ttLL$) jets. By means of a template fitting procedure, the inclusive $ttcc$, $ttbb$, and $ttLL$ cross sections are simultaneously measured, together with their ratios to the inclusive $tt + 2$ jets cross section. This provides measurements of the $ttcc$ and $ttbb$ cross sections of $8.0 \pm 1.1\,(\text{stat.}) \pm 1.3\,(\text{syst.})$ pb and $4.09 \pm 0.34\,(\text{stat.}) \pm 0.55\,(\text{syst.})$ pb, respectively, in the full phase space. The results are consistent with expectations from the Standard Model. The results are presented in Fig. 9 for different combinations of cross sections or ratios.

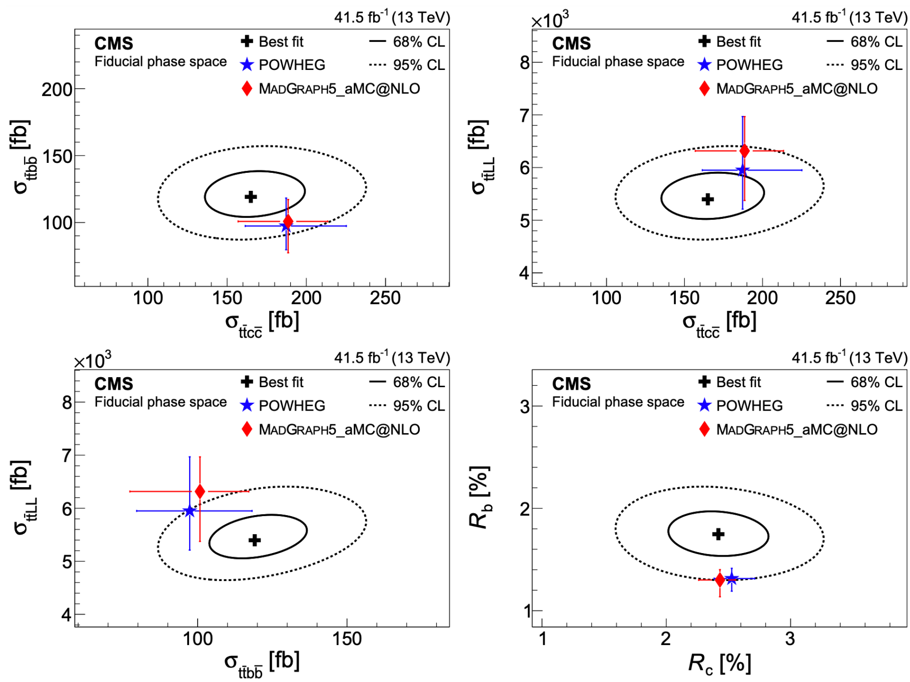

Fig. 9. Results of two-dimensional likelihood scans for different combinations of cross sections or ratios [11].

3. Higgs sector results

3.1. H mass measurement

CMS presented updated results for the measurement of the Higgs boson mass in the diphoton decay channel, based on the 2016 dataset. A refined detector calibration and new analysis techniques are used to improve the precision of this measurement (see Section 1). The Higgs boson mass is measured to be $m_H = 125.78 \pm 0.26$ GeV. These results are then combined with the ZZ to 4 lepton final state and with previous measurements, leading to the currently most precise value: $m_H = 125.38 \pm 0.14$ GeV, see Fig. 10 [12].

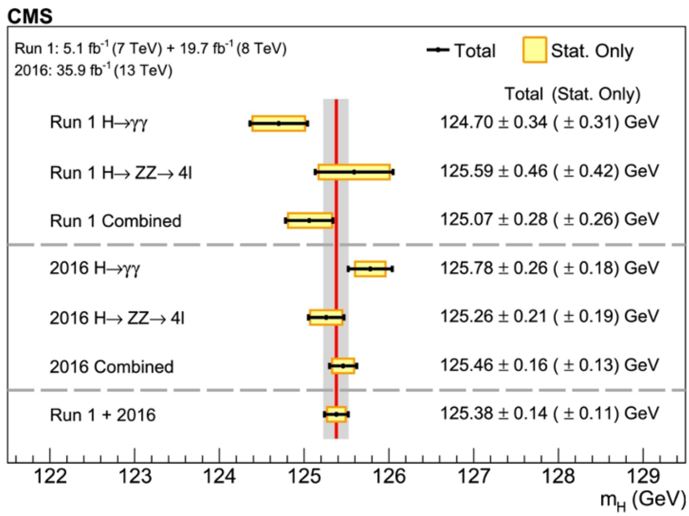

Fig. 10. The updated CMS Higgs boson mass measurement [12].

3.2. H couplings to fermions

If the Run 1 data allowed for the H boson discovery via its decay channel to bosons, the large Run 2 dataset was needed to measure the direct H coupling to the third generation of fermions. Indeed the first observation of H decay to tau leptons happened in summer 2017 [13], the associated production with a top quark in spring 2018 [14], and the H decay to bottom quarks in summer 2018 [15]. The next challenge is to measure the H coupling to the second generation. The H decay to a charm-quark pair is a very challenging channel, with a large background contribution from H decay to b-quark pairs. The latest CMS results on this channel obtained an observed (exp.) upper limit on the signal strength parameter $\mu < 70(37)$ [16].

A key CMS result of summer 2020 is the observation of the H decay channel to a muon pair, see Ref. [17]. It is a rare decay with a branching fraction of 2×10^{-4}, and with a large, irreducible background from the Drell–Yan process. Four production channels are considered: ggH, VBF (vector boson fusion), VH and ttH, the highest cross section being for the ggH and VBF production. The BDT output in the case of the ggH category is presented in Fig. 11 (left). The dimuon invariant mass distribution is presented in Fig. 11 (right). An excess of events over the background expectation (without the H boson) is observed in data with a significance of 3.0σ, where the SM expectation for a H mass of 125.38 GeV is 2.5σ. The combined signal strength parameter is measured to be $\mu = 1.19 \pm^{0.40}_{0.39}$ (stat.)$\pm^{0.15}_{0.14}$ (syst.). Figure 12 (left) presents the μ values for the 4 categories separately. The best fit estimates for the reduced coupling modifiers compared to their corresponding SM prediction are shown in Fig. 12 (right).

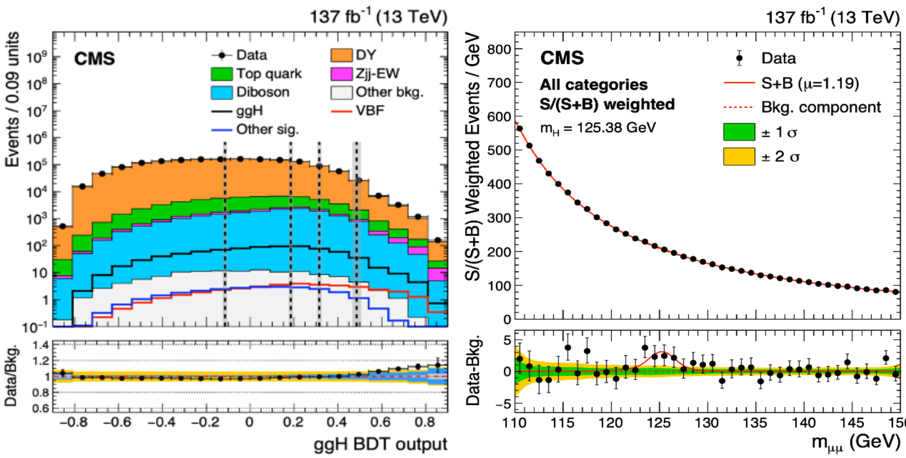

Fig. 11. Left: the observed BDT output distribution compared to the SM background simulations, for the ggH category; Right: the dimuon invariant mass distribution for the weighted combination of all the event categories [17].

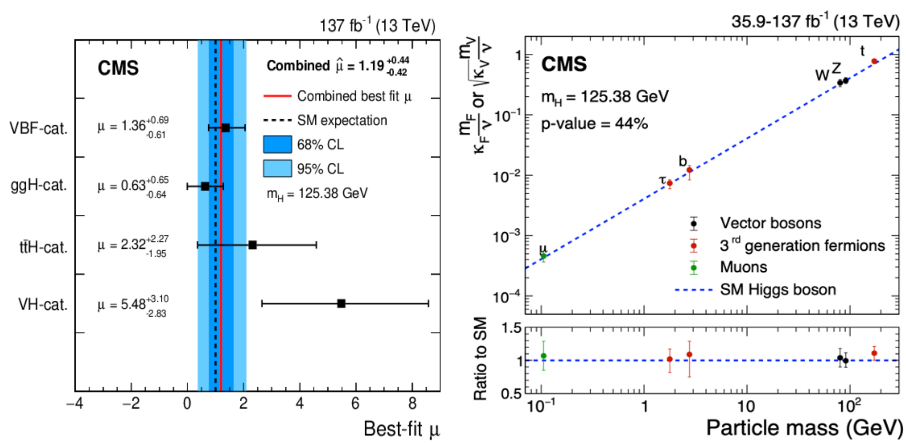

Fig. 12. Left: signal strength measured for $m_H = 125.38$ GeV in each production category compared to the SM expectation; Right: the best fit estimates for the reduced coupling modifiers compared to their corresponding SM prediction [17].

3.3. H to $\gamma\gamma$

The recent full Run 2 results on the measurement of the H boson production cross sections and couplings in events where the Higgs boson decays into a pair of photons are published in Ref. [18]. Four production modes are considered: ggH, VBF, VH and ttH. The total H boson signal strength is measured to be 1.12 ± 0.09. Other properties of the Higgs boson are measured, including production cross sections and its couplings to other particles, precise measurements of ggH and VBF H boson production in several different kinematic regions, the first measurement of ttH production in five regions of the H boson transverse momentum.

The analysis is designed to enable measurements within the simplified template cross section (STXS) framework [19]. The STXS framework provides a coherent approach with which to perform precision Higgs boson measurements. Its goal is to minimise the theory dependence of Higgs boson measurements, both in lessening the direct impact of SM predictions on the results and in providing access to kinematic regions likely to be affected by BSM physics. Two different measurements are performed within this framework, in which 17 and 27 independent kinematic regions are measured simultaneously, with corresponding p-values with respect to the SM of 31 and 70%, respectively, see Fig. 13.

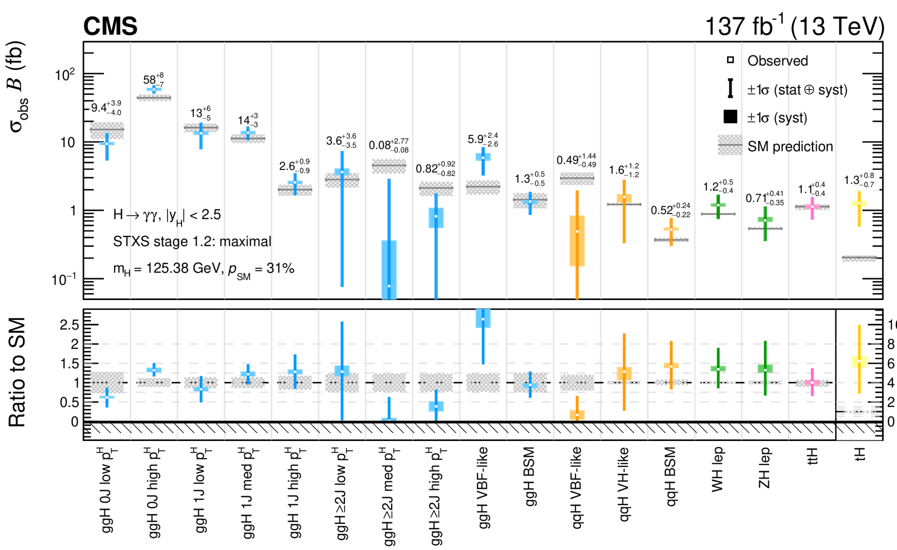

Fig. 13. Results of the cross section production in the STXS framework [18].

3.4. H to ττ

Recent full Run 2 results on H boson production in the channel where the H boson decays to τ leptons are published in [20]. The signal strength is measured to be 0.85 ± 0.12. Measurements of the signal strengths and products of the cross section and branching fraction are also performed in the STXS scheme, providing precise measurements of the H boson production at high transverse momentum and in event topologies with jets. All results are compatible with the SM expectation.

3.5. Boosted H to bb

A search for SM H bosons produced with transverse momentum (p_{T}) greater than 450 GeV and decaying to bottom quark–antiquark pairs (bb) is detailed in Ref. [21]. Highly Lorentz-boosted H bosons decaying to bb are reconstructed as single large-radius jets, and are identified using jet substructure and a dedicated b tagging technique based on a deep neural network. The method is validated with the Z to bb events. For a Higgs boson mass of 125 GeV, an excess of events above the background assuming no Higgs boson production is observed with a local significance of 2.5σ, while the expectation is 0.7, see Fig. 14 (left). The corresponding signal strength is $\mu = 3.7\pm^{1.6}_{1.5}$. Additionally, an unfolded differential cross section as a function of H boson p_{T} is measured, see Fig. 14 (right).

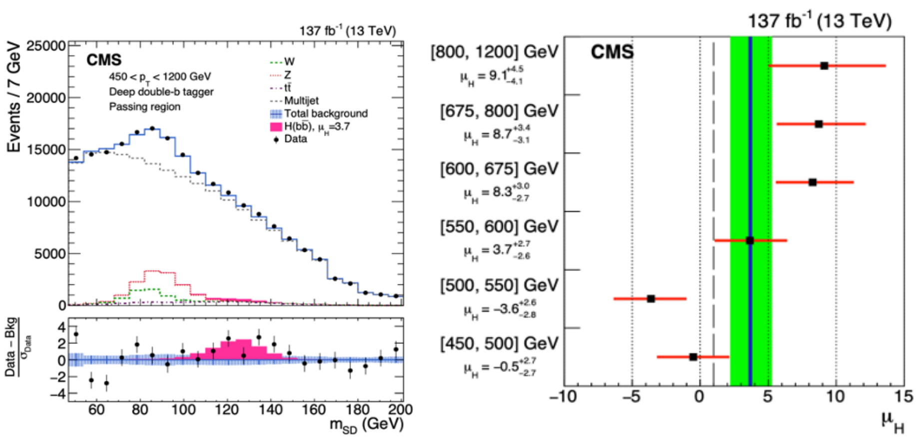

Fig. 14. Left: the observed and fitted background bb-invariant mass distributions for the DBT passing region, combining all the p_{T} categories; Right: signal strength value and uncertainty per p_{T} category [21].

4. Direct searches for new physics

Recent results of direct searches for new physics are presented in this section. Two new SUSY results are described: the electroweak and strong production with dilepton final states, and the stop-quark pair production in dilepton final states. It is followed by the search for long-lived particles decaying into displaced jets and, finally, the search for dark photons in vector boson fusion (VBF) production is presented.

4.1. Search for supersymmetric particules

A search for BSM phenomena in final states with two oppositely charged same-flavour leptons and MET has been performed on the full Run 2 data [22]. Three potential signatures of new physics are explored: an excess of events with a lepton pair, whose invariant mass is consistent with the Z boson mass; a kinematic edge in the invariant mass distribution of the lepton pair; and the nonresonant production of two leptons, see Fig. 15 (left). The observed event yields are consistent with the SM expectation. The results are used to set upper limits on the production cross sections of simplified models of supersymmetry (SUSY). The results of the first search allow the exclusion of gluino masses up to 1870 GeV, as well as chargino (neutralino) masses up to 750 (800) GeV, while those of the searches for the other two signatures allow the exclusion of light-flavour (bottom) squark masses up to 1800 (1600) GeV and slepton masses up to 700 GeV (see Fig. 15 (right)), respectively, at 95% confidence level (C.L.) within certain SUSY scenarios.

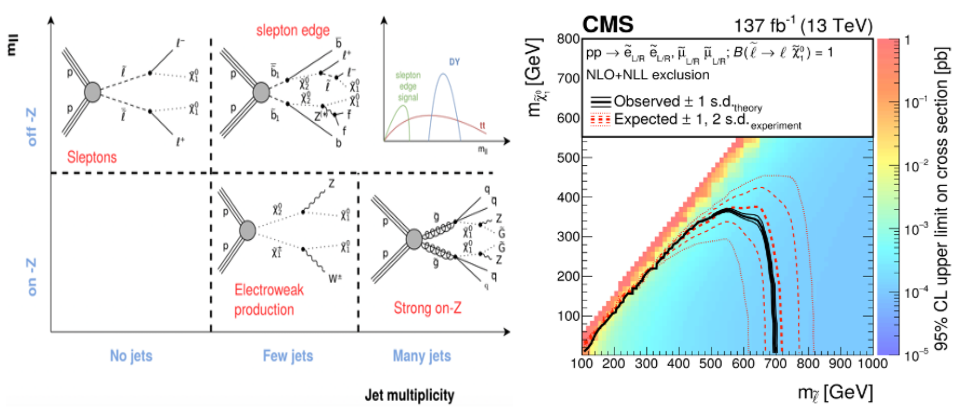

Fig. 15. Left: diagrams considered in the analysis for various jet multiplicity and for an on-Z or off-Z selection for the dilepton invariant mass; Right: cross section upper limits and exclusion contours at 95% C.L. for an SMS model of slepton-pair production as a function of the slepton and the lightest neutralino masses [22].

Another recent SUSY CMS result concerns the search for top-squark pair production in final states with two opposite-charge leptons, b jets, and significant MET, using the full Run 2 dataset [23]. Transverse mass variables and the significance of MET are used to efficiently suppress backgrounds from SM processes. No evidence for a deviation from the expected background is observed and the results are interpreted in several simplified models for supersymmetric top-squark pair production and decay. For top squarks decaying exclusively to a top quark and a lightest neutralino, lower limits are placed at 95% C.L. on the masses of the top squark and the neutralino up to 925 and 450 GeV, respectively. If the decay proceeds via an intermediate chargino, the corresponding lower limits on the mass of the lightest top squark are set up to 850 GeV for neutralino masses below 420 GeV. For top squarks undergoing a cascade decay through charginos and sleptons, the mass limits reach up to 1.4 TeV and 900 GeV respectively for the top squark and the lightest neutralino.

4.2. Search for long-lived particles

Numerous BSM scenarios propose the existence of long-lived particles (LLPs) that have macroscopic decay lengths, as for an example split SUSY, SUSY with weak R-parity violation, SUSY with gauge-mediated SUSY breaking (GMSB), dark matter models. It is common for the LLPs to further decay into final states containing jets, giving rise to displaced-jets signatures. CMS has performed an inclusive search for LLP using displaced jets, example of BSM diagrams being shown in Fig. 16 (left). Standard and displaced triggers are used targeting a mean proper decay lengths $c\tau$ displacement from 1 mm to 10 m. Machine learning techniques are included

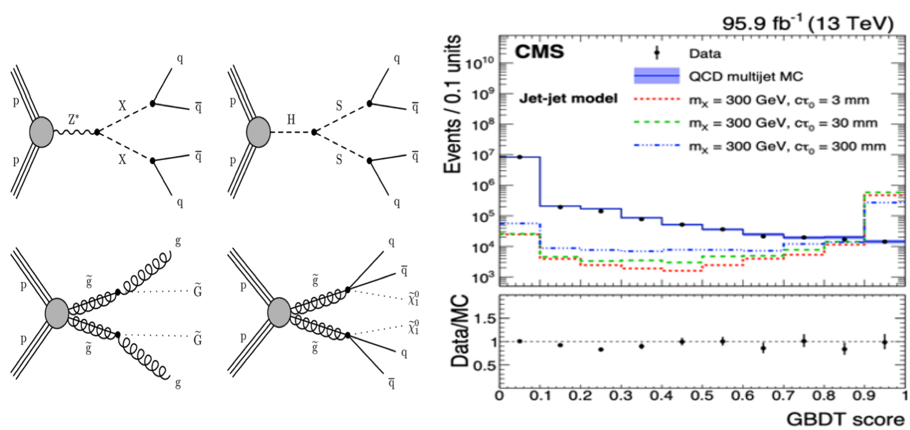

Fig. 16. Left: Example of BSM diagrams leading to LLP decay; Right: BDT score result in the case of the jet–jet model analysis [24].

to improve the signal-to-background ratio. The BDT output in the case of the jet–jet model (simplified model, where pair-produced long-lived neutral particles decay into quark–antiquark pairs) analysis is presented in Fig. 16 (right). In this case, pair production cross sections larger than 0.07 fb are excluded at 95% C.L. for LLP masses larger than 500 GeV and $c\tau$ between 2 and 250 mm. More interpretation results are given in Ref. [24]. A dedicated analysis optimised for $c\tau$ between 100 μm and 15 mm is detailed in Ref. [25].

4.3. Search for dark photon in VBF production

This last subsection presents a first analysis on the Higgs boson that is produced via VBF and that decays to an undetected particle and an isolated photon, using the full Run 2 dataset [26]. Events with 2 forward high-p_{T} jets, large MET and an isolated high-p_{T} photon are selected. Several control regions are defined to constrain the background contributions. No significant excess of events above the expectation from the SM background is found. Figure 17 (left) presents the transverse mass distribution for the signal region with dijet mass above 1500 GeV. The results are interpreted in the context of a theoretical model in which the undetected particle is a massless dark photon. The upper limit on the product of the cross section for production via VBF and the branching fraction for such a Higgs boson decay is shown in Fig. 17 (right), as a function of the H boson mass. For a Higgs boson mass of 125 GeV, assuming the SM production rates, the observed (exp.) 95% C.L. upper limit on the branching fraction is 3.5 (2.8)%. Combination with a previous search for Higgs bosons produced in association with a Z boson results in an observed (exp.) upper limit on the branching fraction of 2.9 (2.1)% at 95% C.L.

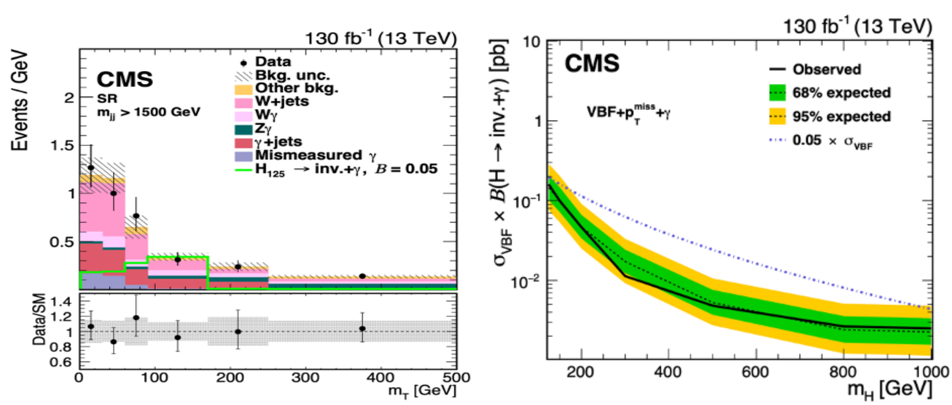

Fig. 17. Left: transverse mass distribution; Right: observed and expected upper limits at 95% C.L. on the product of σ_{VBF} and B ($H \to$ inv. $+\,\gamma$) as a function of the H mass [26].

5. CMS activities during LS2 and plans for the Run 3

During the Long Shutdown 2 (LS2), in years 2019–2021, the collaboration provides important efforts to the maintenance and the improvement of the CMS detector, as well as the implementation of the phase 1 upgrade. In addition, several activities were performed dedicated to the phase 2 (High Luminosity LHC, HL-LHC) upgrades and related services and infrastructure. A summary of these activities is presented in Fig. 18.

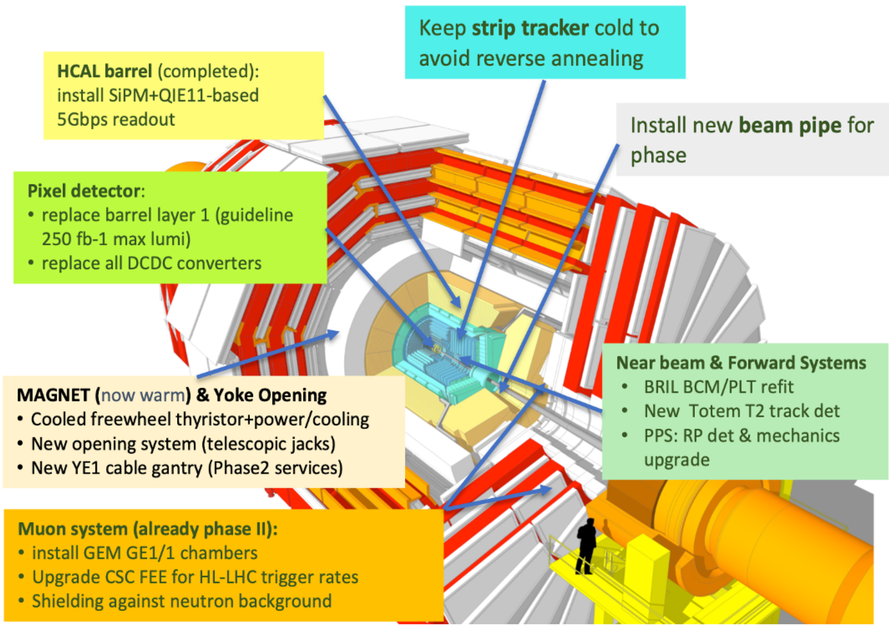

Fig. 18. Maintenance and upgrade activities performed on the CMS detector during the Long Shutdown 2 in years 2019–2021.

It is interesting to notice that only a small delay has been accumulated during the LS2 due to the COVID-19 pandemic, and the LHC machine is still planned to restart in February 2022. All CMS LS2 activities will be performed in time for the first short test beam foreseen at the end of 2021. The collaboration is presently preparing the Run 3 (2022–2024), for which an integrated luminosity of about 250 fb^{-1} is expected to be taken, more than doubling the present LHC statistics. The schedule of the LHC machine is shown in Fig. 19.

Fig. 19. LHC schedule including the Run 1 and Run 2 as well as the future Run 3 and the High-Lumi (HL-LHC) phase.

6. Conclusions

The year 2020 was particularly difficult in the world due to the COVID-19 pandemic. However, impressive CMS results were published using the full Run 2 dataset, presenting various first important measurements. In the case of SM measurement, a first result on the polarised same-sign WW cross section was obtained as well as the first observation of the $VVV*$ production, of the electroweak $W\gamma$ production, of the top-pair production together with a charm-quark pair. In the Higgs sector, the highlight came from the summer 2020 results with the evidence of the very rare process of $H \to \mu\mu$ decay, accessing the H coupling to the second generation of fermions. Concerning BSM, final legacy results are being published using the full Run 2 dataset and placing strong constrains on various models of new physics, in particular probing difficult final state as long-lived particles with displaced vertex. It is worth to notice that VBF production is now widely considered. Machine learning algorithms are implemented in many analyses for signal selection and background rejection, as well as in object reconstruction or trigger. With the coming Run 3 data and the high luminosity phase, LHC physicists have still many years of data to be collected and analysed in the future.

REFERENCES

[1] CMS Collaboration (S. Chatrchyan *et al.*), «The CMS experiment at the CERN LHC», *JINST* **03**, S08004 (2008).

[2] CMS Collaboration (A.M. Sirunyan *et al.*), «Reconstruction of signal amplitudes in the CMS electromagnetic calorimeter in the presence of overlapping proton–proton interactions», *JINST* **15**, P10002 (2020), `arXiv:2006.14359 [physics.ins-det]`.

[3] CMS Collaboration (A.M. Sirunyan *et al.*), «Electron and photon reconstruction and identification with the CMS experiment at the CERN LHC», *JINST* **16**, P05014 (2021), `arXiv:2012.06888 [hep-ex]`.

[4] CMS Collaboration, «Performance of Electron and Photon reconstruction in the 2017 Legacy dataset of the CMS Experiment», CMS-DP-2020-024, May 2020, `https://cds.cern.ch/record/2718815`

[5] CMS Collaboration, «Performance of the DeepTau algorithm for the discrimination of taus against jets, electron, and muons», CMS-DP-2019-033, Oct 2019, `http://cds.cern.ch/record/2694158`

[6] CMS Collaboration, «Performance of the DeepJet b tagging algorithm using 41.9/fb of data from proton–proton collisions at 13 TeV with Phase 1 CMS detector», CMS-DP-2018-058, `https://cds.cern.ch/record/2646773`

[7] CMS Collaboration, «Measurements of production cross sections of polarized same-sign W boson pairs in association with two jets in proton–proton collisions at $\sqrt{s} = 13$ TeV», *Phys. Lett. B* **812**, 136018 (2021), `arXiv:2009.09429 [hep-ex]`.

[8] CMS Collaboration, «Observation of electroweak production of $W\gamma$ with two jets in proton–proton collisions at $\sqrt{s} = 13$ TeV», *Phys. Lett. B* **811**, 135988 (2020), `arXiv:2008.10521 [hep-ex]`.

[9] CMS Collaboration, «Evidence for electroweak production of four charged leptons and two jets in proton–proton collisions at $\sqrt{s} = 13$ TeV», *Phys. Lett. B* **812**, 135992 (2021), `arXiv:2008.07013 [hep-ex]`.

[10] CMS Collaboration (A.M. Sirunyan *et al.*), «Observation of the Production of Three Massive Gauge Bosons at $\sqrt{s} = 13$ TeV», *Phys. Rev. Lett.* **125**, 151802 (2020), `arXiv:2006.11191 [hep-ex]`.

[11] CMS Collaboration, «First measurement of the cross section for top-quark pair production with additional charm jets using dileptonic final states in pp collisions at $\sqrt{s} = 13$ TeV», `arXiv:2012.09225 [hep-ex]`, submitted to *Phys. Lett. B*.

[12] CMS Collaboration, «A measurement of the Higgs boson mass in the diphoton decay channel», *Phys. Lett. B* **805**, 135425 (2020), `arXiv:2002.06398 [hep-ex]`.

[13] CMS Collaboration, «Observation of the Higgs boson decay to a pair of τ leptons with the CMS detector», *Phys. Lett. B* **779**, 283 (2018), `arXiv:1708.00373 [hep-ex]`.

[14] CMS Collaboration (A.M. Sirunyan *et al.*), «Observation of $t\bar{t}H$ Production», *Phys. Rev. Lett.* **120**, 231801 (2018), arXiv:1804.02610 [hep-ex].

[15] CMS Collaboration (A.M. Sirunyan *et al.*), «Observation of Higgs boson decay to bottom quarks», *Phys. Rev. Lett.* **121**, 121801 (2018), arXiv:1808.08242 [hep-ex].

[16] CMS Collaboration (A.M. Sirunyan *et al.*), «A search for the Standard Model Higgs boson decaying to charm quarks», *J. High Energy Phys.* **2003**, 131 (2020), arXiv:1912.01662 [hep-ex].

[17] CMS Collaboration (A.M. Sirunyan *et al.*), «Evidence for Higgs boson decay to a pair of muons», *J. High Energy Phys.* **2101**, 148 (2021), arXiv:2009.04363 [hep-ex].

[18] CMS Collaboration (A.M. Sirunyan *et al.*), «Measurements of Higgs boson production cross sections and couplings in the diphoton decay channel at $\sqrt{s} = 13$ TeV», *J. High Energy Phys.* **2107**, 027 (2021), arXiv:2103.06956 [hep-ex].

[19] LHC Higgs Cross Section Working Group (D. de Florian *et al.*), «Handbook of LHC Higgs cross sections 4: Deciphering the nature of the Higgs sector», *CERN Yellow Rep. Monogr.* **2**, 1 (2017), arXiv:1610.07922 [hep-ph].

[20] CMS Collaboration, «Measurement of Higgs boson production in the decay channel with a pair of τ leptons», CMS-PAS-HIG-19-010.

[21] CMS Collaboration (A.M. Sirunyan *et al.*), «Inclusive search for highly boosted Higgs bosons decaying to bottom quark–antiquark pairs in proton–proton collisions at $\sqrt{s} = 13$ TeV», *J. High Energy Phys.* **2012**, 085 (2020), arXiv:2006.13251 [hep-ex].

[22] CMS Collaboration (A.M. Sirunyan *et al.*), «Search for supersymmetry in final states with two oppositely charged same-flavor leptons and missing transverse momentum in proton–proton collisions at $\sqrt{s} = 13$ TeV», *J. High Energy Phys.* **2104**, 123 (2021), arXiv:2012.08600 [hep-ex].

[23] CMS Collaboration (A.M. Sirunyan *et al.*), «Search for top squark pair production using dilepton final states in pp collision data collected at $\sqrt{s} = 13$ TeV», *Eur. Phys. J. C* **81**, 3 (2021), arXiv:2008.05936 [hep-ex].

[24] CMS Collaboration, «Search for long-lived particles using displaced jets in proton–proton collisions at $\sqrt{s} = 13$ TeV», arXiv:2012.01581 [hep-ex], submitted to *Phys. Rev. D*.

[25] CMS Collaboration, «Search for long-lived particles decaying to jets with displaced vertices», CMS-PAS-EXO-19-013.

[26] CMS Collaboration (A.M. Sirunyan *et al.*), «Search for dark photons in Higgs boson production via vector boson fusion in proton–proton collisions at $\sqrt{s} = 13$ TeV», *J. High Energy Phys.* **2103**, 011 (2021), arXiv:2009.14009 [hep-ex].